Journal of Mechanical and Construction Engineering, 2025,
Vol. 05, Iss. 01, S. No. 084, pp. 1-22
ISSN (Online): 2583-0619

Advanced Pile Foundation Design for Disaster Resilience Using Best Worst Method and Computational Modeling

Gitartha Kalita[1], Palash Jyoti Hazarika[2]

[1]PhD research scholar, Assam Engineering College, Jalukbari, Guwahati, Assam, India 781013
[2]Professor, Assam Engineering College, Jalukbari, Guwahati, Assam, India 781013
gitartha04-17.cephd@aec.ac.in; gitartha.kalita56@gmail.com

How to cite this paper: G. Kalita, P. J. Hazarika, "Advanced Pile Foundation Design for Disaster Resilience Using Best Worst Method and Computational Modeling," *Journal of Mechanical and Construction Engineering (JMCE), Vol. 05, Iss. 01, S. No. 084*, pp. 1–22, 2025.

https://doi.org/10.54060/a2zjournals.jmce.84

Received: 09/01/2025
Accepted: 12/03/2025
Online First: 25/04/2025
Published: 25/04/2025

Abstract

The load transfer behavior at the pile-soil interface is essential for ensuring the stability and resilience of pile foundations, particularly in disaster-prone regions. The allowable load a pile can bear depends on factors such as soil type, pile dimensions, and the interaction between the pile and surrounding soil, all of which are critical in maintaining structural integrity during seismic events, floods, and other natural disasters. This study investigates these complexities, proposing innovative approaches to accurately calculate load transfer and optimize disaster resilience strategies. An extensive review of three decades of literature identified six foundational studies on load transfer equations. Load-settlement curves were generated using Octave software, accommodating various soil types and pile dimensions commonly encountered in disaster scenarios. To refine calculations, codes were developed to compute allowable bearing loads using formulas from the Indian Standard code. A decision tree model implemented in Python further predicted the optimal calculation methods for specific conditions under disaster stress scenarios.

Additionally, the research explored six distinct methods for evaluating allowable loads: Point by Point Curve, Cubic Root Curve, Hiramaya Curve, Hyperbolic Curve, Krasinski Curve, and Root Curve. Among these, the Hiramaya Curve emerged as the most con-servative and reliable, offering a higher factor of safety due to its lower allowable load estimates. To enhance accuracy, weightages for each method were evaluated using the Best Worst Method (BWM), offering a systematic framework for prioritizing the methods based on their reliability and effectiveness. The findings revealed significant variations in load-bearing capacities across soil types and pile dimensions, emphasizing the necessity of site-specific designs. A novel code was also developed to streamline optimal load calculation methods, improving the efficiency, reliability, and disaster resilience of pile foundation designs. This comprehensive framework equips geotechnical engineers with adaptable tools and robust methodologies to design saf-

er, more resilient structures across diverse geotechnical conditions.

Keywords

Load transfer behavior, Best Worst Method, Pile-soil interface, Octave software, Decision tree model, Optimal load calculation methods

1. Introduction

Foundations are vital for providing support, stability, and safety to buildings, ensuring compliance with regulations [1]. It can be categorized into shallow and deep foundations, each with its own advantages and limitations, selected based on soil con-ditions, site characteristics, and structural requirements. Pile foundations, a type of deep foundation, are crucial for transfer-ring loads from structures to deeper, more stable soil or rock layers [2]. Piles, typically made of concrete, steel, or timber, offer increased bearing capacity, stability, resistance to lateral loads, and cost-effectiveness, especially in weak or high-water-table soil conditions [3].

1.1. Load Settlement Behavior

Pile foundation settlement stems from factors like soil consolidation, pile compression, and elastic pile deformation [4]. Un-derstanding these settlements (including elastic, consolidation, secondary consolidation, differential, tilting, and heave set-tlement) is pivotal for ensuring structural integrity and safety. Immediate settlement, primarily for piles in sand, and consoli-dation settlement, especially for saturated clay soils, play significant roles. Analyzing settlement behavior helps predict set-tlement, prevent failures, ensure compliance, and optimize costs [5-6].

Load transfer in pile-soil systems involves numerous parameters like soil type, pile length, and diameter. Accurately assessing these parameters is challenging but essential for rational pile foundation design [7]. The load-transfer curve, depicting pile-soil interaction, is crucial for evaluating load-settlement response. Various methods, including empirical and numerical approaches, help in constructing load-settlement curves which help to ensure structural stability and longevity [8]. Previous studies have proposed different approaches for analyzing load-settlement curves, considering soil types, pile materials, and installation methods [9-10]. These studies have developed various curve types, including linear, root, trilinear, hyperbolic, point by point, and cubic root curves, each suited to specific soil and pile characteristics as sown in Table 1.

Table 1. Details of various studies related to load vs settlement curve

Curve	Soil type	Pile type			Reference
		Material of Construction	Method of installation	Mode of Load Transfer	
Linear curves	Sand (Loose/ Medium/ Dense), Clay (Loose/ Medium/ Dense).	Timber, Steel, Concrete, Composite piles	Driven, Bored, Vibrated, Jetted	Bearing, Friction, Tension	[11]
Root curve	Sand (Loose/ Medium/ Dense)	Timber, Steel, Concrete, Composite piles	Driven	Bearing, Friction, Tension	[12]
Linear curves	Fine-grained soil and Coarse-grained soil	Timber, Steel, Concrete, Composite piles	Replacement piles and Driven piles	Bearing, Friction, Tension	[13]

Trilinear curves	Sand (Loose/ Medium/ Dense), Clay (Loose/ Medium/ Dense).	Timber, Steel, Concrete, Composite piles	Driven, Bored, Vibrated, Jetted	Bearing, Friction, Tension	[14-15]
Hyperbolic curves	Sand (Loose/ Medium/ Dense), Clay (Loose/ Medium/ Dense).	Timber, Steel, Concrete, Composite piles	Driven, Bored, Vibrated, Jetted	Bearing, Friction, Tension	[16]
Point by point curves	Clay non-Carbonate sand.	Timber, Steel, Concrete, Composite piles	Driven, Bored, Vibrated, Jetted	Bearing, Friction, Tension	[17]
Cubic root curve	Sand (Loose/ Medium/ Dense), Clay (Loose/ Medium/ Dense).	Timber, Steel, Concrete, Composite piles	Driven, Bored, Vibrated, Jetted	Bearing, Friction, Tension	[18]
Hyperbolic curve	Sand (Loose/ Medium/ Dense), Clay (Loose/ Medium/ Dense).	Timber, Steel, Concrete, Composite piles	Driven, Bored, Vibrated, Jetted	Bearing, Friction, Tension	[18]

1.2. Literature review

Reference [9] introduced an analytical approach to establish theoretical load-settlement curves for piles loaded in clay, va-li-dating their method through both field and laboratory experiments. Reference [6] employed Mindlin's equation to examine settlement behavior, emphasizing the prevalence of immediate settlement in ideal soil conditions. Reference [19] developed closed-form solutions for piles loaded vertically in linear elastic soil, while [20] proposed a method for calculating shaft and end resistance in piles driven into sand. Several researchers suggested methodologies for predicting settlement [21-23], demonstrating favorable agreement with field tests. Reference [24] introduced a method for assessing load settlement be-havior similar to that of [9]. The studies synthesized the load settlement curve at the pile's top by numerically integrating load transfer relationships. Reference [25] derived a semi-empirical equation for settlement ratio in sand, while [8] outlined a procedure for t-z curves along bored piles. Recent studies by [18] and [26] introduced cubic, hyperbolic, and trilinear load transfer models, enhancing accuracy in load-settlement predictions.

Reference [27] proposed a methodology for determining load deformation and distribution curves for bored piles in residual weathered formation, incorporating nonlinear behavior of pile material. Reference [28] used a load transfer approach to evaluate load distribution and deformation of drilled shafts, proposing a hyperbolic model for shear function. Reference [29] proposed a variational approach for analyzing vertical deformation of pile groups, predicting performance reasonably well. Reference [30] studied the response of piles in calcareous sand under lateral loading, proposing load transfer curves believed to offer an improved approach for pile design. The authors modified the two most common methods used in practice, which are described in detail by [31] and [17] based on [32]. Reference [33] evaluated the accuracy of prediction models for pile settlement in the UAE, recommending suitable models [34-35] for different loading stages. Results showed that settlement values predicted by [34] and [35] overestimated the true values. However, it was observed that Vesic method was less conservative than the Poulos method. Reference [36] used p-y and t-z curves to study the response of offshore platforms [36], modeling static and dynamic curves using nonlinear springs and dashpots. Reference [37] developed a methodology to account for stress relief and soaking of boreholes in water, proposing a modulus reduction factor for load transfer curves. Reference [38] presented a modified analytical model for analyzing pile axial load capacity, using solid finite elements with nonlinear load transfer curves. Reference [39] demonstrated earth-pile reaction under subsidence conditions using t-z and q-z curves. Reference [40] developed normalized equations for axially loaded piles based on an elastoplastic soil model. Reference [41] interpreted load transfer curves from static load tests on large-diameter pipe piles in silty soils. Reference [42] presented t-z and q-z curves based on instrumented bored piles in layered soils, using calibrated modulus for accurate load settlement prediction. The developed curve has little difference from the t-z curve for clay [43]. Reference [44] proposed a methodology for determining load transfer and settlement curves, accommodating nonlinear soil stress-strain behavior. Reference [45] introduced static t-z curves for suction caissons in marine sand, suggesting implementation in preliminary foundation design. Reference [46] analyzed load-transfer behavior of prestressed concrete test piles, proposing empirical models and calibrating stiffness parameters.

The importance of load transfer curves in analyzing pile behavior under axial and lateral loads has grown significantly, leading to improved predictive capabilities. In India, load settlement behavior is primarily assessed through field tests, with limited consideration given to theoretical load settlement curves. Theoretical curves are essential, particularly in situations where field tests are impractical, necessitating reliance on static pile load formulas. Thus, there arises a necessity for theoretical load settlement curves in India, in addition to improving codal provisions. Considering these requirements, an attempt is made to perform a comparative study of the applicability of load transfer theories proposed by various researchers and predict pile behavior based on them. This study aims to refine pile foundation design accuracy by comparing various load transfer theories and aligning numerical predictions with field test results, which will enhance design reliability, investigate new construction materials and techniques, and broaden parameters for future research.

2. Methodology

The framework of the study is illustrated in Figure 1. Initially, an extensive literature review was conducted in the relevant field. Subsequently, six studies were selected for analysis. Each of these studies presented two equations for calculating the load transfer curve, which characterizes the behavior of the pile-soil interface along both the pile shaft and the pile tip. Uti-lizing these equations, load-settlement curves were derived for each study. Consequently, a code was developed based on these equations to generate load-settlement curves, taking into account various pile dimensions and soil types. Following the development of these codes, the allowable bearing load was computed for each soil type using the formula given in the Indian Standard code. Upon determining the load capacities for each soil type, a new code was developed to determine the optimal method for load calculation. This innovative code streamlines the process by allowing users to input pile dimensions and soil types, thereby generating the most accurate load calculation method by using GNU Octave. To enhance the analysis, each study's weightage is evaluated using the best-worst method (BWM) for each type of soil based on the calculated allowable load. The procedure of BWM is given in Annexure I.

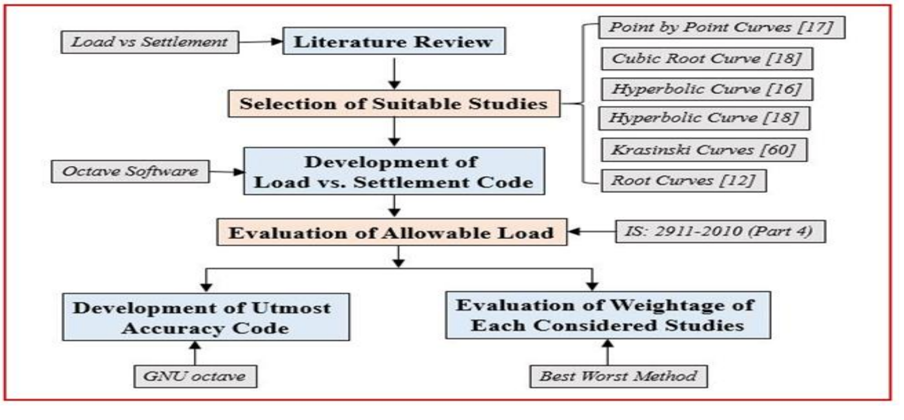

Figure 1. Framework of the study

3. Experimental Results

3.1. Load vs settlement

The details of typical lengths and capacities of various pile types are shown in Table 2 [47]. This information is used only as a guideline in the initial planning and analysis stages.

Table 2. Details of typical lengths and capacities

Pile Type	Pile Length (m)		Approximate Design load (kN)	
	Usual Range	Maximum	Usual Range	Maximum
Timber	10 to 18	30	150 to 200	300
Driven Precast Concrete	10 to 15	30	300 to 600	900
Driven Prestressed Concrete	20 to 30	60	500 to 600	900
Cast in situ concrete (Drilled Shell)	15 to 25	40	300 to 750	900
Concrete cast in situ bulb piles	15 to 25	45 (large dia)	600 to 3000	9000 (large dia)
Steel Pipe	20 to 40	Unlimited	300 to 1000 (small dia)	2500 to 10000 (large dia)
Composite	20 to 40	60	300 to 900	2000

The table presents a comparative analysis of various types of piles, including their usual and maximum lengths, as well as their approximate design loads. Timber Piles typically have a usual length ranging from 10 to 18 meters, with a maximum length of 30 meters. These piles offer a moderate design load capacity, ranging from 150 to 200 kN in the usual range and reaching a maximum of 300 kN. Timber piles are commonly used in applications where moderate loads are expected, such as marine construction projects. Driven Precast Concrete Piles are known for their durability and ease of installation. They have a usual length ranging from 10 to 15 meters, with a maximum length of 30 meters. The design load capacity of precast concrete piles is significantly higher than timber piles, ranging from 300 to 600 kN in the usual range and reaching a maximum of 900 kN. Driven Prestressed Concrete Piles offer even higher load-bearing capacities compared to precast concrete piles. With a usual length ranging from 20 to 30 meters and a maximum length of 60 meters, these piles can withstand design loads ranging from 500 to 600 kN in the usual range, with a maximum of 900 kN. Cast in situ Concrete (Drilled Shell) Piles are constructed on-site and offer versatility in terms of length and load capacity. With a usual length ranging from 15 to 25 meters and a maximum length of 40 meters, these piles can withstand design loads ranging from 300 to 750 kN in the usual range and up to 900 kN maximum. Concrete Cast in situ Bulb Piles are designed for heavy-duty applications, offering exceptional load-bearing capacities. With a usual length of 15 to 25 meters and a maximum length of 45 meters for large diameters, these piles can support design loads ranging from 600 to 3000 kN in the usual range, reaching a maximum of 9000 kN for large diameter piles. Steel Pipe Piles are characterized by their versatility and durability. With a usual length ranging from 20 to 40 meters and unlimited maximum length, steel pipe piles can accommodate a wide range of design loads. Small diameter piles can support loads ranging from 300 to 1000 kN, while large diameter piles can withstand loads ranging from 2500 to 10000 kN. Composite Piles offer a balance between load-bearing capacity and versatility. With a usual length ranging from 20 to 40 meters and a maximum length of

60 meters, these piles can support design loads ranging from 300 to 900 kN in the usual range, with a maximum of 2000 kN.

For this study, the various parameters of the soil such as bearing capacity factor (Nq), earth pressure coefficient (K), internal friction angle (Ø), unit weight (ɣ), and pile soil friction angle (δ), were obtained by taking reference of Indian Standard Code 2911 as shown in Table 3 and Table 4 [48]. The pile material used is the concrete pile. The value of δ for the driven pile is obtained from Indian Standard Code 2911. Five different diameters (B) and lengths (L) of concrete piles were considered for the analysis as shown in Table 5.

Table 3. Values of K (earth pressure coefficient) and δ

Pile material	δ	K for loose sand	K for dense sand
Steel	20	0.5	1.0
Concrete	0.75Ø	1.0	2.0
Timber	0.67Ø	1.5	4.0

Table 4. The different soil parameters and their sources, which were used for driven piles.

Type of sand	Nq	K	Ø	ɣ	δ
Silty sand	55	1.2	35	18	30
Loose sand	17	1	25	11	18.8
Uniform sand	60	1.5	35	17.3	26.3
Medium sand	22	1	27	18	20.25
Dense sand	137	2	40	18	30
Fine sand	68	1	36	17.3	27

Table 5. Dimension of Pile

Sl. No.	Diameter in m (B)	Length in m (L)	References
1	0.5	12	[47]
2	0.2	8	
3	0.25	12	
4	0.45	20	
5	0.45	9	

In this analysis, a total 6 number of studies related to load transfer curves are selected as shown in **Table 6**. Additionally, 6 types of soil conditions are considered such as uniform sand, loose sand, medium sand, dense sand, fine sand, and silty sand soil.

Table 6. Selected Studies of the analysis

Sl. No.	Name of the curve	References
1	Point by point curves	[17]
2	Cubic root curve	[18]
3	Hyperbolic Curve	[16]
4	Hyperbolic Curve	[18]

5	Krasinski	[49]
6	Root curve	[12]

These load transfer curves were considered since the other load transfer curves required some additional values such as pressure-meter modulus, shear modulus, the radius of influence, and Poisson's ratio, which are difficult to obtain at times. The load transfer curves that were considered had minimum requirements and were very convenient to use. After the selection of 5 classes for pile dimensions and 6 types of soil conditions, load vs settlement codes are developed using octave software. Here under each type of soil there are 5 classes of pile dimensions, and under each class of pile dimension there are 6 studies which gives equations for load vs settlement curve. Therefore, in this study, total 180 load vs settlement curves are developed. The outcome of Point by point curve (for dense sandy soil, length 8m and diameter 0.2m) is shown in **Figure 2**.

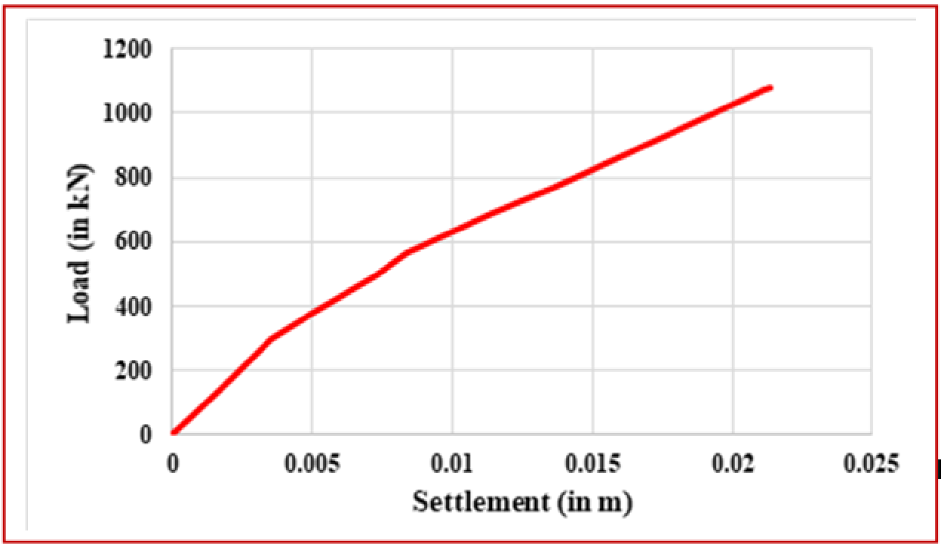

Figure 2. Load vs settlement for dense sand, B is 0.2m and L is 8m using API

3.2. Allowable Load Calculations

According to IS: 2911-1974 (Part 4), the allowable load may be taken as minimum of (a) 0.67 times final load at 12mm settlement or (b) 0.5 times of load at a point where settlement values is 10% of the pile diameter. So, after the development of 180-load vs settlement curves, the loads at 12 mm settlement and loads required to give settlement, which is equal to 10% of pile diameter, are extracted for each curve. Using the extracted information from each curve, the allowable load for driven piles for various cases (various pile types, pile dimensions, and considered studies) is calculated. The evaluated allowable load for various cases are shown in Tables 7 to 11. These tables provides a comparison of loads at different settlement levels for various types of sands (silty, loose, uniform, medium, fine, and dense) under different conditions of B and L. The loads are compared across different studies represented by various curve such as point by point curves, cubic root curve, Hiramaya curve, hyperbolic curve, Krasinski, and root curve.

Table 7. Allowable load for B = 0.5m and L = 12m

Studies	Load at 12mm settlement	Load at 10% pile diameter settlement	Allowable load
Silty sand			
Point by point curves	2654.30	3397.30	1698.65
Cubic root curve	2184.20	3587.80	1456.13
Hiramaya curve	1323.30	2187.60	882.20

Hyperbolic curve	2431.30	3587.80	1620.87
Krasinski	2095.90	3496.20	1397.27
Root curve	2129.80	3004.40	1419.87
Loose sand			
Point by point curves	669.85	817.40	408.69
Cubic root curve	692.10	817.40	408.69
Hiramaya curve	415.22	817.40	276.81
Hyperbolic curve	679.65	817.40	408.69
Krasinski	585.17	817.40	390.12
Root curve	2157.20	3199.10	1438.13
Uniform sand			
Point by point curves	2757.9	3736.6	1836.6
Cubic root curve	2267.1	3736.6	1511.4
Hiramaya curve	1471.1	3736.6	985.73
Hyperbolic curve	2526.9	3736.6	1684.6
Krasinski	2181.6	3736.6	1454.4
Root curve	2157.2	3199.1	1438.13
Medium sand			
Point by point curves	1314	1528.1	876
Cubic root curve	1292.7	1601.3	861.8
Hiramaya curve	2666.3	1601.3	1067.53
Hyperbolic curve	1270.3	1601.3	846.87
Krasinski	1087.8	1586.9	725.2
Root curve	1153.3	1367.9	768.87
Dense sand			
Point by point curves	2937.7	7374.6	1958.47
Cubic root curve	2217.5	7903.1	1478.3
Hiramaya curve	2440	7903.1	1626.67
Hyperbolic curve	3182.7	7903.1	2121.8
Krasinski	2095.4	7166.3	1396.93
Root curve	2188.1	6449.9	1458.73
Fine sand			
Point by point curves	2550.3	3442	1700.2
Cubic root curve	2004	3659.5	1336
Hiramaya curve	1091.9	3659.5	727.93
Hyperbolic curve	2353.6	3659.5	1569.07
Krasinski	2008.1	3616.8	1338.73
Root curve	1986.5	3050.4	1324.33

Table 8. Allowable load for B = 0.2m and L = 8m

Studies	Load at 12mm settlement	Load at 10% pile diameter settlement	Allowable load
Medium sand			
Point by point curves	170.27	172.90	86.45
Cubic root curve	175.16	176.59	88.30
Hiramaya curve	176.59	176.59	88.30
Hyperbolic curve	168.93	176.59	88.30
Krasinski	153.13	176.59	88.30

Root curve	163.07	164.14	82.07
Fine sand			
Point by point curves	263.07	271.4	135.7
Cubic root curve	274.75	283.47	141.74
Hiramaya curve	175.73	283.47	117.15
Hyperbolic curve	258.82	283.47	141.74
Krasinski	231.53	277.67	138.84
Root curve	240.44	250.99	125.50
Dense sand			
Point by point curves	400.21	425.22	212.61
Cubic root curve	412.69	451.88	225.94
Hiramaya curve	193.54	451.88	129.03
Hyperbolic curve	389.88	451.88	225.94
Krasinski	333.84	426.67	213.34
Root curve	353.12	374.38	187.19
Loose sand			
Point by point curves	118.98	114.48	82.86
Cubic root curve	168.94	170.95	85.47
Hiramaya curve	170.95	170.95	85.47
Hyperbolic curve	160.11	170.95	85.47
Krasinski	146.11	170.95	85.47
Root curve	184.51	186.98	93.49
Uniform sand			
Point by point curves	653.02	697.7	348.85
Cubic root curve	553.03	735.43	367.72
Hiramaya curve	406.67	735.43	272.46
Hyperbolic curve	631.59	735.43	367.72
Krasinski	514.28	694.89	344.56
Root curve	500.38	649.44	324.72
Silty sand			
Point by point curves	634.97	669.53	354.41
Cubic root curve	525.87	707.82	353.91
Hiramaya curve	390.33	707.82	260.22
Hyperbolic curve	521.35	707.82	304.24
Krasinski	521.83	656.17	347.89
Root curve	520.88	614.48	307.24

Table 9. Allowable load for B = 0.45m and L = 9m

Studies	Load at 12mm settlement	Load at 10% pile diameter settlement	Allowable load
Loose sand			
Point by point curves	1519.3	4892.9	1017.93
Cubic root curve	518.89	611.24	305.62
Hiramaya curve	292.29	611.24	195.83
Hyperbolic curve	1840.9	6490.2	1233.4
Krasinski	450.81	608.21	302.04
Root curve	579.04	692.39	346.19
Medium sand			

Point by point curves	1032.4	1148.5	574.25
Cubic root curve	1027.8	1206.9	603.45
Hiramaya curve	523.67	1206.9	350.85
Hyperbolic curve	1000.7	1206.9	603.45
Krasinski	876.01	1193.9	586.92
Root curve	883.54	1017.9	508.95
Fine sand			
Point by point curves	2081.7	2654.7	1387.8
Cubic root curve	2057.6	2844.5	1371.73
Hiramaya curve	798.45	2844.5	532.3
Hyperbolic curve	2035.9	2844.5	1357.27
Krasinski	1659.8	2725.6	1106.53
Root curve	1766.9	2351.1	1175.6
Silty sand			
Point by point curves	1048.20	1177.90	588.95
Cubic root curve	1035.00	1228.20	614.10
Hiramaya curve	6519.00	1228.20	614.10
Hyperbolic curve	1018.20	1228.20	614.10
Krasinski	8508.70	1204.60	602.30
Root curve	9003.10	1045.20	522.60
Uniform sand			
Point by point curves	842.63	954.49	477.25
Cubic root curve	834.64	1005.50	502.75
Hiramaya curve	408.59	1005.50	272.39
Hyperbolic curve	813.74	1005.50	502.75
Krasinski	969.20	994.21	497.11
Root curve	727.07	860.42	430.21
Dense sand			
Point by point curves	1480.10	1801.9	900.95
Cubic root curve	1447.30	1928.5	964.87
Hiramaya curve	490.90	1928.5	327.27
Hyperbolic curve	1405.40	1928.5	936.93
Krasinski	1200.30	1874.0	800.20
Root curve	1204.40	1536.2	768.10

Table 10. Allowable load for B = 0.45m and L = 20m

Studies	Load at 12mm settlement	Load at 10% pile diameter settlement	Allowable load
Loose sand			
Point by point curves	1063.3	2262.2	712.41
Cubic root curve	812.47	921.95	460.97
Hiramaya curve	596.65	921.95	399.75
Hyperbolic curve	1032.6	2956.2	691.84
Krasinski	667.23	909.54	447.04
Root curve	868.73	1003.1	501.55
Medium sand			
Point by point curves	1474.3	1692.4	846.2
Cubic root curve	1136.6	1757.9	761.52

Hiramaya curve	1052	1757.9	704.84
Hyperbolic curve	1276.6	1757.9	855.32
Krasinski	1097.6	1706.2	735.39
Root curve	1109	1568.8	743.03
Fine sand			
Point by point curves	1629.7	3327.8	1091.7
Cubic root curve	1145.3	3575.9	767.35
Hiramaya curve	1383.2	3575.9	922.13
Hyperbolic curve	1721.4	3575.9	1147.6
Krasinski	1139.4	3230.5	759.6
Root curve	1114.7	3082.5	743.13
Silty sand			
Point by point curves	1714	3556.2	1142.47
Cubic root curve	1109	3771.5	739.33
Hiramaya curve	1671.7	2637.4	1114.47
Hyperbolic curve	1858.9	3771.5	1239.27
Krasinski	1160.1	3480.8	773.4
Root curve	1093.5	3298.9	729
Uniform sand			
Point by point curves	1746	3690.8	1164
Cubic root curve	1040.5	3075.7	693.67
Hiramaya curve	739.3	3916.6	492.87
Hyperbolic curve	1860.9	3632.6	1240.6
Krasinski	2300.6	3589.7	1533.73
Root curve	2192.4	3481.3	1461.6
Dense sand			
Point by point curves	1490	4973.9	993.6
Cubic root curve	1044.9	3055.5	696.60
Hiramaya curve	2372.9	4908.4	1581.93
Hyperbolic curve	17779.6	5748.6	11853.067
Krasinski	1039.3	3715.2	692.87
Root curve	992.9	3192.3	661.93

Table 11. Allowable load for B = 0.25m and L = 12m

Studies	Load at 12mm settlement	Load at 10% pile diameter settlement	Allowable load
Loose sand			
Point by point curves	491.99	882.45	329.63
Cubic root curve	284.57	298.5	149.25
Hiramaya curve	207.69	298.5	139.15
Hyperbolic curve	450.12	904.84	301.58
Krasinski	241.13	295.06	147.53
Root curve	306.44	323.54	161.77
Medium sand			
Point by point curves	520.61	546.99	273.49
Cubic root curve	523.16	567.28	283.64
Hiramaya curve	366.11	567.28	245.29
Hyperbolic curve	511.72	567.28	283.64

Krasinski	440.03	552.32	276.16
Root curve	476.05	508.94	254.47
Silty sand			
Point by point curves	794.06	1141.9	264.69
Cubic root curve	546.71	1058.5	182.24
Hiramaya curve	652.10	860.46	217.4
Hyperbolic curve	879.64	1126.2	293.21
Krasinski	551.64	1107.6	183.88
Root curve	580.5	1064.6	193.50
Uniform sand			
Point by point curves	812.32	1184.6	541.55
Cubic root curve	599.55	1076.1	399.7
Hiramaya curve	1530.5	1724.5	862.25
Hyperbolic curve	886.77	1163.9	581.95
Krasinski	565.45	1148.7	376.97
Root curve	557.15	1122.3	371.43
Fine sand			
Point by point curves	827.56	1054.9	527.45
Cubic root curve	560.1	1058.8	373.4
Hiramaya curve	521.92	1136.5	347.95
Hyperbolic curve	839.58	1036.9	518.45
Krasinski	574.27	1017.1	382.85
Root curve	568.507	984.22	379.00
Dense sand			
Point by point curves	925.88	1491.9	617.3
Cubic root curve	523.67	1104.4	349.1
Hiramaya curve	1040.7	1559.2	693.8
Hyperbolic curve	932.72	1651.7	621.8
Krasinski	588.17	1098.5	392.1
Root curve	576.56	1119.1	384.4

The loads vary significantly across different settlement levels, indicating the sensitivity of the soil to applied loads. For example, at 12mm settlement, the loads are generally lower compared to the loads at 10% pile diameter settlement. Different types of sands exhibit distinct load-bearing capacities. For instance, dense sand generally has higher load-bearing capacities compared to loose or fine sand. This aligns with the expected behavior, as denser sands typically offer better support due to their compactness. The dimensions of the B and L also play a crucial role in determining the load-bearing capacity. For example, when comparing the same type of sand with different base dimensions, it can be observed variations in load-bearing capacities. A larger diameter or length generally results in higher load-bearing capacities. Different curve yield slightly different results. For instance, while the point by point curves and hyperbolic curve may provide similar results for some soil types, there could be variations in others. This indicates the importance of selecting an appropriate curve technique based on the specific soil characteristics and project requirements. The reliability and accuracy of the results depend on various factors such as the quality of data, appropriateness of the curve technique, and representativeness of the soil samples. Engineers and researchers need to consider these factors while interpreting and utilizing the results for practical applications. The table's data can be valuable for geotechnical engineers, foundation designers, and construction professionals involved in designing and analyzing pile foundations. It helps them understand the expected behavior of different types of sands under varying conditions and make informed decisions during the design process.

Following the determination of the allowable load in each scenario, a novel code has been devised using decision tree algorithm [50-51]. This code serves to furnish precise guidance when supplied with input data concerning piles and soil properties. Essentially, by inputting relevant details regarding the soil type and pile characteristics, the code can discern and recommend the most optimal methods for computing the allowable load under those specific conditions. In essence, this code streamlines the process of selecting the most effective methodology tailored to the given soil-pile configuration. By harnessing this tool, engineers and practitioners can expedite the determination of allowable loads with heightened accuracy, thereby enhancing the efficiency and reliability of pile foundation design endeavors.

To validate the efficacy of the newly developed code, a series of inputs were systematically fed into the system. These inputs encompassed a range of soil and pile configurations, representing diverse conditions encountered in practical engineering contexts. Upon processing the input data, the code autonomously determined the most conservative method for calculating the allowable load under each specific set of circumstances. In this study, the conservative approach is selected because greater safety will be ensured. For instance, for a pile, according to Study A and Study B, allowable loads of 100kN and 150kN are reported, respectively. It is understood that the allowable load indicates the maximum load a pile can withstand. Therefore, opting for Study A, with its 100kN limit, ensures a higher level of safety compared to selecting the 150kN limit from Study B. This is due to the fact that these load values are assumptions within the studies, thus favoring a lower load for enhanced safety. Hence, in this study, the conservative method is employed, which prioritizes the study providing the lowest allowable load. The results of this analysis, including the input details and the recommended method, are meticulously documented in Table 12 to 16. In these tables, C is cohesion factor, α is adhesion factor, E is modulus of elasticity and the final column denoted as P signifies the output generated by the developed code. Each row corresponds to a unique combination of input parameters, including soil type, pile dimensions, and other pertinent factors. The recommended method for calculating the allowable load is indicated alongside each set of input parameters. Specifically, the abbreviations HI, KR, API, CU, and VI represent [16], [49], [17], [18] and [12], respectively.

Through this comprehensive validation process, engineers and practitioners can gain confidence in the reliability and accuracy of the developed code. By aligning with established methodologies and expert recommendations, the code serves as a valuable tool for expediting pile foundation design while ensuring optimal performance and safety in various geotechnical contexts.

Table 12. Conservative method to calculate allowable load for B=0.5m and =12m

Nq	K	Ø	δ	ɣ	C	α	E	P
55	1.2	35	30	18	0	0	21000000	HI
17	1	25	18.8	11	0	0	21000000	HI
68	1	36	27	17.3	0	0	21000000	HI
60	1.5	25	26.3	17.3	0	0	21000000	HI
22	1	27	20.25	18	0	0	21000000	HI
137	2	40	30	18	0	0	21000000	KR
55	0.47	32	32	18	0	0	21000000	VI
17	0.62	22	22	11	0	0	21000000	HI
68	0.45	33	33	17.3	0	0	21000000	HI

60	0.47	32	32	17.3	0	0	21000000	VI
22	0.59	24	24	18	0	0	21000000	HI
137	0.39	37	37	18	0	0	21000000	HI

Table 13. Conservative method to calculate allowable load for B=0.2m and =8m

Nq	K	Ø	δ	γ	C	α	E	P
55	1.2	35	30	18	0	0	21000000	HI
17	1	25	18.8	11	0	0	21000000	API
68	1	36	27	17.3	0	0	21000000	HI
60	1.5	25	26.3	17.3	0	0	21000000	HI
22	1	27	20.25	18	0	0	21000000	HI
137	2	40	30	18	0	0	21000000	CU
55	0.47	32	32	18	0	0	21000000	VI
17	0.62	22	22	11	0	0	21000000	API
68	0.45	33	33	17.3	0	0	21000000	HI
60	0.47	32	32	17.3	0	0	21000000	VI
22	0.59	24	24	18	0	0	21000000	HI
22	0.59	24	24	18	0	0	21000000	VI

Table 14. Conservative method to calculate allowable load for B=0.45m and =9m

Nq	K	Ø	δ	γ	C	α	E	P
55	1.2	35	30	18	0	0	21000000	HI
17	1	25	18.8	11	0	0	21000000	HI
68	1	36	27	17.3	0	0	21000000	HI
60	1.5	25	26.3	17.3	0	0	21000000	HI
22	1	27	20.25	18	0	0	21000000	HI
137	2	40	30	18	0	0	21000000	HI
55	0.47	32	32	18	0	0	21000000	VI
17	0.62	22	22	11	0	0	21000000	CU
68	0.45	33	33	17.3	0	0	21000000	HI
60	0.47	32	32	17.3	0	0	21000000	HI
22	0.59	24	24	18	0	0	21000000	HI
137	0.39	37	37	18	0	0	21000000	HI

Table 15. Conservative method to calculate allowable load for B=0.45m and =20m

Nq	K	Ø	δ	ɣ	C	α	E	P
55	1.2	35	30	18	0	0	21000000	VI
17	1	25	18.8	11	0	0	21000000	API
68	1	36	27	17.3	0	0	21000000	CU
60	1.5	25	26.3	17.3	0	0	21000000	CU
22	1	27	20.25	18	0	0	21000000	HI
137	2	40	30	18	0	0	21000000	VI
55	0.47	32	32	18	0	0	21000000	HI
17	0.62	22	22	11	0	0	21000000	KR
68	0.45	33	33	17.3	0	0	21000000	HI
60	0.47	32	32	17.3	0	0	21000000	HI
22	0.59	24	24	18	0	0	21000000	VI
137	0.39	37	37	18	0	0	21000000	HI

Table 16. Conservative method to calculate allowable load for B=0.25m and =12m

Nq	K	Ø	δ	ɣ	C	α	E	P
55	1.2	35	30	18	0	0	21000000	HI
17	1	25	18.8	11	0	0	21000000	HI
68	1	36	27	17.3	0	0	21000000	HI
60	1.5	25	26.3	17.3	0	0	21000000	VI
22	1	27	20.25	18	0	0	21000000	HI
137	2	40	30	18	0	0	21000000	VI
55	0.47	32	32	18	0	0	21000000	HI
17	0.62	22	22	11	0	0	21000000	KR
68	0.45	33	33	17.3	0	0	21000000	HI
60	0.47	32	32	17.3	0	0	21000000	HI
22	0.59	24	24	18	0	0	21000000	VI
137	0.39	37	37	18	0	0	21000000	HI

The table provides a comprehensive overview of various soil and pile configurations along with corresponding parameters and the methodology used for calculation. The parameters listed include B, L, Nq, K, Ø, δ, ɣ, C, α, and E, representing different aspects of soil and pile characteristics. Additionally, the methodology column specifies the method employed for calculating the parameters. Certain methods, such as the HI and CU, are frequently utilized across different soil and pile configurations. Parameters such as Nq, K, Ø, and δ exhibit variation across different configurations, indicating the influence of soil type and pile dimensions on these characteristics. The choice of methodology can significantly affect parameter values, as evidenced by variations in calculated parameters under different methods for similar configurations. By selecting the most appropriate method for calculation based on specific soil and pile characteristics, engineers can optimize parameter values to enhance the accuracy of foundation design and analysis. The developed code undergoes validation by manually determining the allowable load under specified soil and pile conditions, utilizing a comprehensive selection of studies. Subsequently, analysis reveals that the code advocates a methodology that yields the most conservative outcomes among all considered studies.

3.3. Assigning of Weightage

In this study, the Best-Worst Method (BWM) is utilized to assign weights to six load vs settlement studies based on their corresponding values. This approach ensures that methods with higher values, which represent better performance or greater preference, receive higher weights while maintaining that the total weight sum equals 1 [52]. The provided values for each method serve as the basis for calculating their relative importance. For silty sand (B = 0.5m and L = 12m), it is observed that Study 3 yields the lowest allowable load, whereas Study 1 provides the highest allowable load. A lower allowable load indicates that the structure will bear a minimal load on that soil, making the design inherently safer. Conversely, a higher allowable load implies higher risk, as the soil would be subjected to its maximum capacity. Thus, a study offering the minimum allowable load is considered the best for that soil type, while a study yielding the maximum allowable load is deemed the least favorable. The preference of the best and worst criterion over the other criteria for silty soil (B=0.5m and L=12m) is shown in Annexure II. By evaluating the allowable loads across various soil conditions and studies, the weight of each study has been calculated for different soil types with varying dimensions, as detailed in Tables 17 to 21.

Table 17. Weightage of each study B = 0.5m and L = 12m

Soil Type	S1	S2	S3	S4	S5	S6
Silty Sand	0.0519	0.1038	0.4672	0.0742	0.1731	0.1298
Loose sand	0.1666	0.1666	0.2751	0.1866	0.1639	0.0412
Uniform sand	0.1095	0.1522	0.2111	0.1488	0.1798	0.1986
Medium sand	0.1534	0.1654	0.1244	0.1777	0.1966	0.1825
Danse Sand	0.1134	0.1832	0.1633	0.1792	0.1932	0.1677
Fine Sand	0.1211	0.1624	0.1942	0.1788	0.1833	0.1602

Table 18. Weightage of each study B = 0.2m and L = 8m

Soil Type	S1	S2	S3	S4	S5	S6
Silty Sand	0.1276	0.1467	0.2022	0.1622	0.1833	0.178
Loose sand	0.1211	0.1624	0.1942	0.1788	0.1833	0.1602
Uniform sand	0.1666	0.1666	0.2751	0.1866	0.1639	0.0412
Medium sand	0.1765	0.1592	0.1592	0.1592	0.1592	0.1867
Danse Sand	0.1211	0.1624	0.1942	0.1788	0.1833	0.1602
Fine Sand	0.1642	0.1287	0.2112	0.1287	0.1763	0.1909

Table 19. Weightage of each study B = 0.45m and L = 9m

Soil Type	S1	S2	S3	S4	S5	S6
Silty Sand	0.2098	0.1298	0.1298	0.1298	0.1654	0.2354
Loose sand	0.1134	0.1832	0.1633	0.1792	0.1932	0.1677
Uniform sand	0.1276	0.1467	0.2022	0.1622	0.1833	0.178
Medium sand	0.1211	0.1624	0.1942	0.1788	0.1833	0.1602
Danse Sand	0.1134	0.1832	0.1633	0.1792	0.1932	0.1677
Fine Sand	0.1498	0.1721	0.1693	0.1244	0.1834	0.201

Table 20. Weightage of each study B = 0.45m and L = 20m

Soil Type	S1	S2	S3	S4	S5	S6
Silty Sand	0.1211	0.1624	0.1942	0.1788	0.1833	0.1602
Loose sand	0.1666	0.1666	0.2751	0.1866	0.1639	0.0412
Uniform sand	0.2098	0.1298	0.1298	0.1298	0.1654	0.2354
Medium sand	0.1134	0.1832	0.1633	0.1792	0.1932	0.1677
Danse Sand	0.1534	0.1654	0.1244	0.1777	0.1966	0.1825
Fine Sand	0.1276	0.1467	0.2022	0.1622	0.1833	0.178

Table 21. Weightage of each study B = 0.25m and L = 12m

Soil Type	S1	S2	S3	S4	S5	S6
Silty Sand	0.1534	0.1654	0.1244	0.1777	0.1966	0.1825
Loose sand	0.1211	0.1624	0.1942	0.1788	0.1833	0.1602
Uniform sand	0.1666	0.1666	0.2751	0.1866	0.1639	0.0412
Medium sand	0.1276	0.1467	0.2022	0.1622	0.1833	0.178
Danse Sand	0.1211	0.1624	0.1942	0.1788	0.1833	0.1602
Fine Sand	0.1398	0.1822	0.2011	0.1578	0.1621	0.157

For silty sand, (B = 0.5), the Hirayama Curve has the highest weightage of 0.4672, followed by Root Curve (0.1298). The other curves such as Cubic Root and Point by Point also provide relevant results but with much lower weightages, indicating that for Silty Sand, the Hirayama method offers the most reliable model. As pile dimensions change to B = 0.2 and B = 0.45, the Hirayama Curve continues to dominate the weightage, though the Root Curve becomes more relevant with B = 0.45 (0.2354). Fine Sand shows the greatest variation, where the weightage for the Root Curve increases with larger pile dimensions, suggesting its higher adaptability under these conditions. In loose sand, there is a noticeable shift. For B = 0.5, the Cubic Root Curve and Hirayama Curve show relatively similar weightages, but Hirayama Curve seems to provide a better fit for B = 0.45, with 0.1721 for B = 0.45, L = 20. The Root Curve maintains a lower weightage, which shows that other methods like Cubic Root and Hirayama offer more robust solutions for modeling in Loose Sand. For uniform sand (B = 0.5), the Cubic Root and Hirayama Curve show similar weightages, with Cubic Root slightly outperforming others. As the pile dimension decreases, especially for B = 0.25, the Cubic Root method becomes more useful, with weightages approaching 0.1666. The Point by Point method also performs well in this scenario, but not as strongly as others. In medium sand, the Hyperbolic Curve generally performs well, with a stable weightage across different pile dimensions. B = 0.5 shows a 0.1777 weightage for this curve, while the Root Curve offers more consistent values, which can be beneficial for medium sand types across different pile dimensions. In dense sand, Hirayama Curve has a high weightage in this category, especially for B = 0.2 and B = 0.45, with values around 0.1833. This indicates that Hirayama might be a more accurate model for evaluating pile performance in dense sand, where particle structure and load distribution differ from looser sands. In fine sand, Hirayama and Root Curves emerge as the most relevant methods for Fine Sand, especially as pile dimensions increase. The Root Curve shows a significant rise in weightage with increasing pile dimension, indicating its advantage in predicting pile behavior under such conditions. The Hyperbolic Curve also shows a substantial weightage for B = 0.5, providing valuable insight for soil conditions with finer particles. The Hirayama Curve is the most adaptable across various soil types, especially for Silty Sand and Dense Sand. Its high weightage in these categories suggests that it provides accurate predictions for a broad range of soil conditions and pile dimensions. The Root Curve, while not the top performer across all conditions, provides strong results in some specific scenarios, such as larger pile dimensions in Fine Sand and Silty Sand. The Point by Point and Cubic Root curves provide valuable contributions, particularly in Loose Sand and Uniform Sand conditions. They tend to be more consistent across the data set, though they sometimes fall behind other methods in accuracy. Larger pile dimensions (B = 0.45 and L = 20) generally result in better performance for the Root Curve and Hirayama Curve, while smaller pile dimensions (B = 0.2 and B = 8) tend to favor curves like Cubic Root and Point by Point. This suggests that pile dimension significantly affects the choice of curve for modeling pile behavior, as larger piles may require more complex models that account for deeper penetration and soil interaction. Silty Sand and Fine Sand benefit from the Hirayama Curve, while Loose Sand is more flexible with Cubic Root and Point by Point models. This indicates that understanding the soil type is crucial for selecting the most appropriate curve. For soils like Dense Sand, Medium Sand, and Uniform Sand, the Hyperbolic Curve and Root Curve offer more reliable predictions, indicating the need for these models in granular soils with different levels of compaction.

4. Conclusion

Load transfer curves have proven to be invaluable tools for predicting the relationship between load and settlement values of piles across diverse soil conditions. They offer an initial estimate of pile load capacity, particularly beneficial when pile load testing is impractical. In this study, a thorough review of relevant literature was conducted, followed by the selection of six load transfer curves for further analysis. Subsequently, a code was developed using Octave software, incorporating formulas from each selected study to generate load-settlement curves. These curves were then used to determine allowable loads for varying soil and pile conditions according to Indian standards. Recognizing the time-consuming nature of analyzing a single pile-soil condition with multiple load transfer curves, a new code was developed to identify the most conservative method for calculating allowable loads, streamlining the analysis process.

This study introduces a comprehensive framework for analyzing pile-soil interaction and optimizing load calculation methods. Future research could expand upon this framework by incorporating additional factors influencing load transfer behavior, such as groundwater levels and pile installation techniques. Moreover, further validation of the developed codes with field data could enhance their reliability and applicability. It is essential to acknowledge the limitations of this study, including the reliance on simplified load transfer equations and assumptions inherent in the decision tree model. Additionally, the accuracy of results depends on the quality of input data and the representativeness of soil samples. Nonetheless, the proposed methodology offers valuable insights for geotechnical engineers and foundation designers, aiding informed decision-making in pile foundation design projects.

There remains many opportunities for further exploration and expansion within this project. Currently, the study focuses on concrete piles and driven pile construction methods. However, future endeavors could encompass a wider array of pile types commonly used in construction. Additionally, while the parameters considered in this study include bearing factors

(Nq), angle of internal friction (Ø), angle of pile and soil (δ), coefficient of earth pressure (K), and unit weight of soil (ɣ), future analyses could incorporate additional parameters to improve result accuracy.

Acknowledgements

G. K. thanks Assam Engineering College for providing the laboratory facility

References

[1]. S.C. Dutta, R. Roy, "A critical review on idealization and modeling for interaction among soil–foundation–structure system". *Computers & structures*, Vol. 80, No. 20-21, PP. 1579-1594, 2002.

[2]. L.C. Reese, W.M. Isenhower, S.T. Wang, "*Analysis and design of shallow and deep foundations*", Vol. 10, John Wiley & Sons, 2005.

[3]. H.G. Kempfert, B. Gebreselassie, "Pile foundation", *Excavations and Foundations in Soft Soils*, pp. 349-460, 2006.

[4]. G. G. Meyerhof, "Bearing capacity and settlement of pile foundations"," *Journal of the Geotechnical Engineering Division*, vol. 102, no. 3, pp. 197–228, 1976.

[5]. N. S. Mattes and H. G. Poulos, "Settlement of single compressible pile," *J. Soil Mech. Found. Div.*, vol. 95, no. 1, pp. 189–207, 1969.

[6]. H.G. Poulos, E.H. Davis, "Pile foundation analysis and design", *New York: Wiley*, Vol. 397, pp. 233-248, 1980.

[7]. H. Hirayama, "A unified base bearing capacity formula for piles," *Soils and foundations*, Vol. 28, No. 3, pp. 91-102, 1988.

[8]. H. Zhu, M.F. Chang, "Load transfer curves along bored piles considering modulus degradation", *Journal of Geotechnical and Geoenvironmental Engineering*, Vol. 128, No. 9, pp. 764-774, 2002.

[9]. H.M. Coyle, L.C. Reese, "Load transfer for axially loaded piles in clay", *Journal of the soil mechanics and foundations division*, Vol. 92, No. 2, pp. 1-26, 1966.

[10]. H.M. Coyle, I.H. Sulaiman, "Skin friction for steel piles in sand", *Journal of the Soil Mechanics and Foundations Division*, Vol. 93, No. 6, pp. 261-278, 1967.

[11]. W.D. Guo, M.F. Randolph, "Rationality of load transfer approach for pile analysis", *Computers and Geotechnics*, Vol. 23, No. 1-2, pp. 85-112, 1998.

[12]. V.N. Vijivergiya, "Load-movement characteristics of piles", *In 4th Symp. of Waterway, Port, Coastal and Ocean Div., ASCE*, Vol. 2, pp. 269-284, 1977.

[13]. J.C. Verbrugge, "Évaluation du tassement des pieux à partir de l'essai de pénétration statique", *Revue Française de Géotechnique,* Vol. 15, pp. 75-82, 1981.

[14]. R. Frank, S.R. Zhao, "Estimating the settlement of axially loaded bored piles in fine sand by PMT data", *Liaison LPC*, Vol. 119, 1982.

[15]. R. Frank, "Recent developments in the prediction of pile behavior from pressuremeter tests", *From theory to practice on deep foundations, UFRGS, Porto Alegre, Brazil*, 1985.

[16]. H. Hirayama, "Load-settlement analysis for bored piles using hyperbolic transfer functions", *Soils and Foundations*, Vol. 30, No. 1, pp. 55-64, 1990.

[17]. American Petroleum Institute (API), "Recommended practice for planning, designing, and constructing fixed offshore platforms–Working stress design", *20th Edition, Washington*, DC, 1993.

[18]. C. Bohn, A. Lopes dos Santos, R. Frank, "Development of axial pile load transfer curves based on instrumented load tests", *Journal of Geotechnical and Geoenvironmental Engineering*, Vol. 143, No. 1, pp. 04016081, 2017.

[19]. M.F. Randolph, C.P. Wroth, “Analysis of deformation of vertically loaded piles”, *Journal of the geotechnical engineering division*, Vol. 104, No. 12, pp. 1465-1488, 1978.

[20]. J.L. Briaud, L. Tucker, “Piles in sand: a method including residual stresses”, *Journal of Geotechnical Engineering*, Vol. 110, No. 11, pp. 1666-1680, 1984.

[21]. Y.K. Chow, “Axial and lateral response of pile groups embedded in nonhomogeneous soils”, *International Journal for Numerical and Analytical Methods in Geomechanics*, Vol. 11, No. 6, pp. 621-638, 1987.

[22]. H.G. Poulos, “Analysis of residual stress effects in piles”, *Journal of Geotechnical Engineering*, Vol. 113, No. 3, pp. 216-229, 1987.

[23]. J.M. Polo, J.L. Clemente, “Pile-group settlement using independent shaft and point loads”, *Journal of geotechnical engineering*, Vol. 114, No. 4, pp. 469-487, 1988.

[24]. P.D. Kiousis, A.S. Elansary, “Load settlement relation for axially loaded piles”, *Journal of geotechnical engineering*, Vol. 113, No. 6, pp. 655-661, 1987.

[25]. S.R. Kaniraj, “A semi-empirical equation for settlement ratio of pile foundations in sand”, *Soils and foundations*, Vol. 33, No. 2, pp. 82-90, 1993.

[26]. Z. Zhou, Z. Zhang, C. Chen, F. Xu, T. Xu, L. Zhu, T. Liu, “Application of load transfer method for bored pile in loess area”, *European Journal of Environmental and Civil Engineering*, Vol. 26, No. 10, pp. 4457-4475, 2022.

[27]. E.G. Balakrishnan, A.S. Balasubramaniam, N. Phien-wej, “Load deformation analysis of bored piles in residual weathered formation”, *Journal of geotechnical and geoenvironmental engineering*, Vol. 125, No. 2, pp. 122-131, 1999.

[28]. S. Kim, S. Jeong, S. Cho, I. Park, “Shear load transfer characteristics of drilled shafts in weathered rocks”, *Journal of geotechnical and geoenvironmental engineering*, Vol. 125, No. 11, pp. 999-1010, 1999.

[29]. W.Y. Shen, Y.K. Chow, K.Y. Yong, “A variational approach for the analysis of pile group–pile cap interaction”, *Geotechnique*, Vol. 50, No. 4, pp. 349-357, 2000.

[30]. G.J. Dyson, M.F. Randolph, “Monotonic lateral loading of piles in calcareous sand”, *Journal of Geotechnical and Geoenvironmental Engineering,* Vol. 127, No. 4, pp. 346-352, 2001.

[31]. L.C. Reese, W.R. Cox, F.D. Koop, “Analysis of laterally loaded piles in sand”, *In Offshore Technology Conference*, pp. 2080, OTC, 1974.

[32]. M.W. O’Neill, J.M. Murchinson, “Fan evaluation of py relationships in sands”, *A report to the American Petroleum Institute*, 1983.

[33]. A.S. Al-Homoud, T. Fouad, A. Mokhtar, “Evaluating accuracy for two empirical methods in predicting settlement of drilled shafts”, *Geotechnical & Geological Engineering*, Vol. 22, pp. 245-267, 2004.

[34]. A.S. Vesic, “Design of pile foundations”, *NCHRP synthesis of highway practice*, Vol. 42, 1977.

[35]. H.G. Poulos, “Settlement of single piles in nonhomogeneous soil”, *Journal of the geotechnical engineering division*, Vol. 105, No. 5, pp. 627-641, 1979.

[36]. Y.E. Mostafa, M.H. El Naggar, “Response of fixed offshore platforms to wave and current loading including soil–structure interaction”, *Soil Dynamics and Earthquake Engineering*, Vol. 24, No. 4, pp. 357-368, 2004.

[37]. M.F. Chang, H. Zhu, “Construction effect on load transfer along bored piles”, *Journal of geotechnical and geoenvironmental engineering,* Vol. 130, No. 4, pp. 426-437, 2004.

[38]. H.J. Kim, J.L.C. Mission, I.S. Park, *“Analysis of static axial load capacity of single piles and large diameter shafts using nonlinear load transfer curves”*, *KSCE Journal of Civil Engineering*, Vol. 11, pp. 285-292, 2007.

[39]. K. Hyeongjoo, M. Joseleo, S. Youngsun, B. Jaehong, B. Pilsoon, “Axial Load Capacity Prediction of Single Piles in Clay and Sand Layers Using Nonlinear Load Transfer Curves”, *Journal of the Korean Society of Geotechnical and Environmental Engineering,* Vol. 9, No. 5, pp. 45-52.

[40]. Y.C. Chou, Y.M. Hsiung, "A normalized equation of axially loaded piles in elasto-plastic soil", *Journal of Geotechnical Engineering*, Vol. 4, No. 1, pp. 1-7, 2009.

[41]. A.S. Bradshaw, S. Haffke, C.D. Baxter, "Load transfer curves from a large-diameter pipe pile in silty soil", *In Full-scale testing and foundation design: Honoring bengt h. fellenius*, pp. 590-601, 2012.

[42]. A. Lim, A. Kwanda, P.P. Rahardjo, "The Study of tz and qz curves on Bored Pile Based on The Results of Instrumented Pile Load Test in Medium and Stiff Clays", *Proceedings of Pile*, Vol. 2, No. 4, 2013.

[43]. L.C. Reese, M.W. O'NEIL, "Field load tests of drilled shafts", *In International geotechnical seminar on deep foundations on bored and auger piles*, Vol. 1, pp. 145-191, 1988.

[44]. S. Nanda, N.R. Patra, "Theoretical load-transfer curves along piles considering soil nonlinearity", *Journal of Geotechnical and Geoenvironmental Engineering*, Vol. 140, No. 1, pp. 91-101, 2014.

[45]. S. Grecu, A. Barari, L.B. Ibsen, "Axial Load-Transfer Curves for Suction Bucket Foundations in Sand", *In ISOPE International Ocean and Polar Engineering Conference,* pp. 24-32, 2019.

[46]. M.N. Haque, M. Y. Abu-Farsakh, "Development of analytical models to estimate the increase in pile capacity with time (pile setup) from soil properties", *Acta Geotechnica*, Vol. 14, pp. 881-905, 2019.

[47]. G. Ranjan, A.S.R. Rao, "Basic and applied soil mechanics", *New Age International*, 2011.

[48]. P.K. Jayasree, K.V. Arun, R. Oormila, H. Sreelakshmi, "Lateral load capacity of piles: a comparative study between indian standards and theoretical approach", *Journal of The Institution of Engineers (India): Series A*, Vol. 99, pp. 587-593, 2018.

[49]. A. Krasiński, "Proposal for calculating the bearing capacity of screw displacement piles in non-cohesive soils based on CPT results", *Studia Geotechnica et Mechanica*, Vol. 34, No. 4, pp. 41-51, 2012.

[50]. B. Charbuty, A. Abdulazeez, "Classification based on decision tree algorithm for machine learning", *Journal of Applied Science and Technology Trends*, Vol. 2, No. 1, pp. 20-28, 2021.

[51]. K.K. Rana, "A survey on decision tree algorithm for classification", *International journal of Engineering development and research*, Vol. 2, No. 1, pp. 1-5, 2014.

[52]. J. Rezaei, "Best-worst multi-criteria decision-making method", *Omega*, Vol. 53, pp. 49–57, 2015.

Annexure I: Best Worst Method

A variety of Multi-Criteria Decision-Making (MCDM) methods are available to support decision-making processes, including the Aggregated Indices Randomization Method (AIRM), Analytic Hierarchy Process (AHP), Analytic Network Process (ANP), Fuzzy AHP, Base-Criterion Method (BCM), and Best-Worst Method (BWM), among others. Among these, BWM, introduced by Prof. Rezaei, stands out as an exceptional tool. It requires fewer pairwise comparisons than other methods, leading to more efficient and reliable results while significantly reducing the time needed for analysis. Due to these advantages, BWM has been chosen for this study. This method has been widely applied across various fields. The procedure for implementing this method is outlined below (Rezaei, 2015):

Step 1: The decision criteria for achieving the ultimate objective of the study can be defined as $\{o_1, o_2, o_3 ..... o_n\}$, where each o represents a specific criterion associated with the objective.

Step 2: The decision-maker must identify the best (i.e., most significant) and the worst (i.e., least significant) criteria among all the options.

Step 3: The preference of the best criterion over the other criteria should be assessed using a scale from 1 to 9, where 1 signifies equal preference, and 9 indicates a strong preference. The preferences can be represented as follows:

$$A_B = (a_{b1}, a_{b2}, a_{b3} ....., a_{bn})$$

Step 4: Similarly, the preference of the worst criterion over the other criteria should be evaluated using a scale from 1 to 9, where 1 represents equal preference and 9 signifies strong preference.

$$A_W = (a_{w1}, a_{w2}, a_{w3}....., a_{wn})$$

Step 5: In this step, optimal weights ($w_1^*, w_2^*, w_3^*......., w_n^*$) for each criterion are calculated by ensuring that the conditions w_B/w_j and w_j/w_W. The best possible solution is $w_B/w_j = a_{Bj}$ and $w_j/w_W = a_{jw}$. To obtain these two solutions, maximum among the set of {| w_B-$w_j \times a_{Bj}$ | and | w_j-$w_W \times a_{jw}$ |} should be minimized as follows:

Min, max$_j${| w_B-$w_j \times a_{Bj}$ | and | w_j-$w_W \times a_{jw}$ |}

Subjected to

$$\sum_j w_j = 1, \; w_j \geq 0 \text{ for all } j$$

The equation (i) can be converted into a linear problem as follows:

min, ξ^L

$$\sum_j w_j = 1$$

Subjected to,

$|w_B - a_{Bj} w_j| \leq \xi^L$ for all j

$|w_j - a_{jw} w_W| \leq \xi^L$ for all j

$$\sum_j w_j = 1, \; w_j \geq 0 \text{ for all } j$$

By using the linear problem, the optimal weights of each criterion and ξ^{L^*} can be evaluated.

Annexure II: Preference of the best and worst criterion over the other criteria for Silty Soil (B=0.5m and L=12m).

The preference of the best criterion over the other criteria should be assessed using a scale from 1 to 9, where 1 signifies equal preference, and 9 indicates a strong preference. The preferences can be represented as follows.

BEST	S3	S1	S2	S4	S5	S6
Hirayama curve	1	8	5	7	3	4

Similarly, the preference of the worst criterion over the other criteria should be evaluated using a scale from 1 to 9, where 1 represents equal preference and 9 signifies strong preference.

WORST	*Point by point curves*
Hirayama curve	9
Point by point curves	1
Cubic root curve	3
Hyperbolic curve	2
Krasinski	4